The influence of small scale magnetic field on the polar cap X-ray luminosity of old radio pulsars

Tsygan A.I.[1], Goglichidze O.A.[1], Barsukov D.P.[1,2]

[1] Ioffe Institute [2] SPbSPU

The influence of small-scale magnetic field on the polar cap heating by reverse positrons is considered. The reverse positron current is calculated in the framework of two models: rapid [1] and gradually screening [2]. In the first model only small area above inner gap gives the input to reverse positron current, so reverse current is nearby $10^{-3}-10^{-2}$ of primary electron current. In the case of gradually screening model all areas above inner gap give the input to reverse positron current [3], so reverse current achieves values like $10^{-2}-10^{-1}$ of primary electron current (and in extreme case may become to be comparable with it). To calculate the electron-positron pairs production rate we take into account only the curvature radiation of primary electrons and its absorption in magnetic field. We use the polar cap model with steady space charge limited electron flow.

It is shown that in the case of some old pulsars the model of gradully screening predicts too much strong polar cap heating and too large its X-ray luminosity values which exceeds the total observed X-ray luminosity. But in the case of some other pulsars the model of gradually screening seems may be more appropriate than rapid screening model.

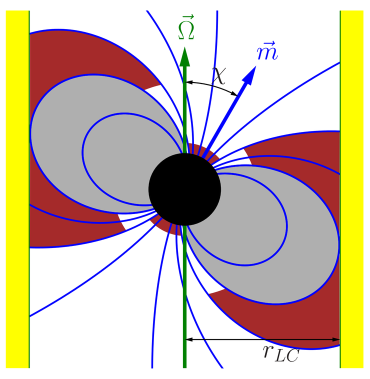

1. Old isolated radiopulsars
   $B_{dip}\sim 10^{11}-10^{12}G$
   $P\sim 100ms-1s$
   $\tau=P/(2\dot P)\gtrsim 10^6$ years
2. Goldreich-Julian model
3. inner gaps
4. free electron emission from neutron star surface
   small surface magnetic field $B_{surf}<10^{13}G$
   hot polar caps $T\sim(1-3)\cdot 10^6K$
   Z.Medin, D.Lai (2007)
   $\vec\Omega\cdot\vec m>0$, $\Omega=\frac{2\pi}{P}$
   $\vec\Omega$ is angular velocity of star
5. no vacuum gaps, no sparks
   steady space charge limited flow
   W.M.Fawley, J.Arons, E.T.Scharlemann (1977)
6. stationary case
7. only curvature radiation
   the inverse compton scattering and synchrotron emission do not taken into account
8. only photon absorption in magnetic field
   no photon splitting, photon scattering

Small scale magnetic field

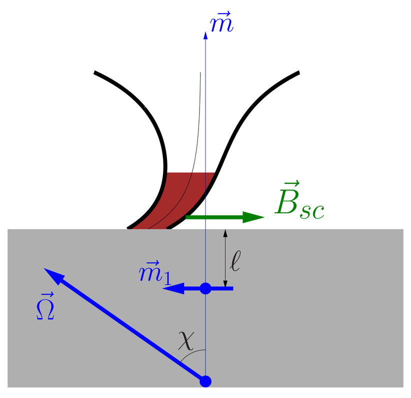

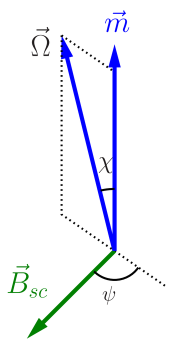

$$\vec B=\frac{3\vec r(\vec r\cdot\vec m)-\vec m r^2}{r^5}+\frac{3\vec\rho(\vec\rho\cdot\vec m_1)-\vec m_1\rho^2}{\rho^5}$$

$$\vec\rho=\vec r-(r_{ns}-\ell)\vec e_z,\quad \vec m=m\vec e_z,\quad \vec m_1=\nu\left(\frac{\ell}{r_{ns}}\right)^3 m\vec e_x$$

$$\ell=\frac{1}{10}r_{ns}\qquad \nu=\frac{B_{sc}}{B_{dip}}\lesssim 1\qquad 0\le\psi\le\frac{\pi}{2}$$

Charge density

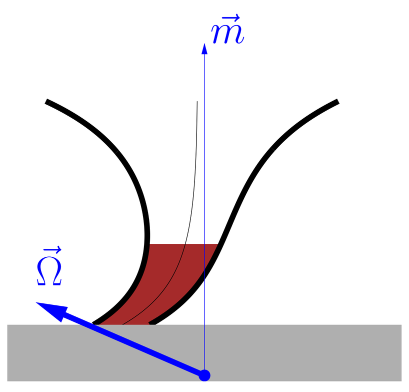

In the reference frame rotating with the star all values do not depend on time.

$$\Delta\Phi=-4\pi(\rho-\rho_{GJ}),\quad \vec E=-\vec\nabla\Phi$$

ρ_{GJ} – Goldreich-Julian density

$$\rho=\frac{\Omega B}{2\pi c}\tilde\rho \quad\text{and}\quad \rho_{GJ}=-\frac{\Omega B}{2\pi c}\tilde\rho_{GJ}$$

$\Omega=2\pi/P$ is angular velocity of neutron star, B is magnetic field strenght

Particles move along field lines $\vec v\parallel\vec B$ with relativistic velocity $v\approx c$

$$\mathrm{div}\,(\rho\vec v)=0 \implies (\vec B\cdot\vec\nabla)\tilde\rho=0$$

without frame dragging

$$\tilde\rho_{GJ}(z)\approx\cos\tilde\chi$$

$\tilde\chi$ is the angle between $\vec B$ and $\vec\Omega$

Rapid screening model

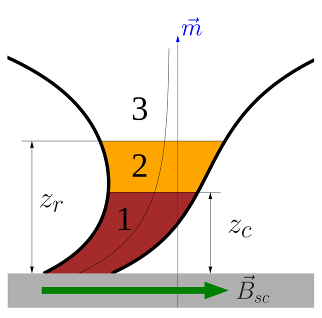

J.Arons, E.T.Scharlemann
ApJ **231** 854 (1979)

1. $0<z<z_c$ acceleration region
   no pairs production, no pair plasma
   large $E_{||}=(\vec E\cdot\vec B)/B$
2. $z_c<z<z_r$ partial screening area
   pair plasma, small $E_{||}$
   positrons return to the polar cap
3. $z>z_r$ full screening area
   pair plasma, $E_{||}=0$
   no positrons return

Condition

(a) $E_{||}\big|_{z=z_r}=0$
electric field is continous

(b) $(\vec B\cdot\vec\nabla)E_{||}\big|_{z=z_r}=0$
charge density is continous

Rapid screening model

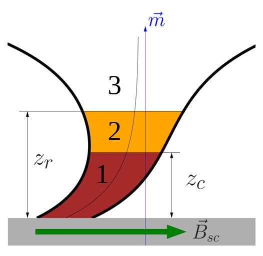

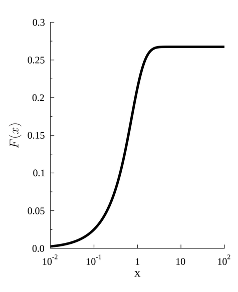

pairs are generated by curvature radiation

$z_r-z_c\ll r_t, z_c$

at $r_t\ll\ell$ at the central line the reverse positron current density may be estimated as

$$\tilde\rho_+\approx r_t\left.\frac{\partial\tilde\rho_{GJ}}{\partial z}\right|_{z=z_c}F\left(\frac{z_c}{r_t}\right)$$

where r_t is the pulsar tube radius, z is altitude above star

$n_+=n_{GJ}\tilde\rho_+$ – number density of the returning positrons

$n_{GJ}=\frac{\Omega B}{2\pi ce}\approx 7\cdot 10^{10}cm^{-3}\left(\frac{1s}{P}\right)\left(\frac{B}{10^{12}G}\right)$

$F(x)\approx\frac{4x}{16+15x}\left(1+1.19\frac{x}{1+x^2}\right)$

$F(x)\approx\frac{x}{4}$ at $x\ll 1$, $F(x)\approx\frac{4}{15}$ at $x\gg 1$

Gradual screening model

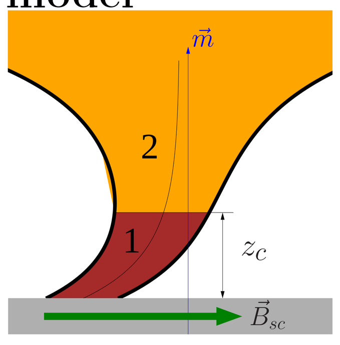

A.K. Harding, A.G. Muslimov
ApJ **556** 987 (2001)

The assumptions:

- all values do not depend on time t (stationary case)
- pairs are affected only by average electric field
- $\tilde\rho_{GJ}$ monotonically grows with the altitude z

Hence, conditions

$E_{||}\big|_{z=z_r}=0$ and $(\vec B\cdot\vec\nabla)E_{||}\big|_{z=z_r}=0$

can not be satisfied at the **same** point

No fullscreening area

There is only partial screening area where the electric field is small and $\Phi\to\Phi_\infty$ at $z\to\infty$

Gradual screening model

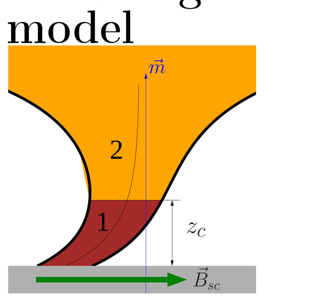

Yu.E. Lyubarskii
A&A **261** 544 (1992)

Returning current from altitude z_f

$$\tilde\rho_+\approx\frac{1}{2}\left(\tilde\rho_{GJ}(z_f)-\tilde\rho_{GJ}(z_c)\right)$$

where $n_+=n_{GJ}\tilde\rho_+$ – number density of returning positrons,

$n_{GJ}=\frac{\Omega B}{2\pi ce}\approx 7\cdot 10^{10}cm^{-3}\left(\frac{1s}{P}\right)\left(\frac{B}{10^{12}G}\right)$

We suppose $z_f\sim(3-15)r_{ns}$

1. $z_f<z_{rad}\sim(5-50)r_{ns}$
   at large z plasma waves affect on pair dynamics
2. $z_f<z_{max}\sim(1-5)r_{ns}$
   where z_{max} is maximum of $\tilde\rho_{GJ}(z)$
   at $z\approx z_{max}$ the solution satisfied both conditions exists
   $E_{||}=0$ and $(\vec B\cdot\nabla)E_{||}=0$

The reverse positron current for pulsar J2043+2740

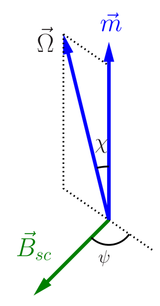

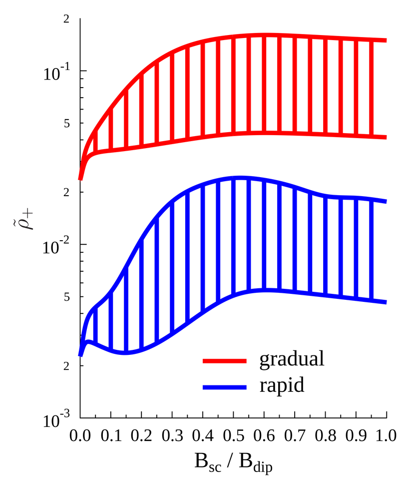

rapid: $\tilde\rho_+\sim 10^{-2}$

$\tilde\rho_+\lesssim r_t\frac{\partial\tilde\rho_{GJ}}{\partial z}$

gradual: $\tilde\rho_+\sim 10^{-1}$

$\tilde\rho_+\approx\frac{1}{2}\left(\tilde\rho_{GJ}(z_f)-\tilde\rho_{GJ}(z_c)\right)$

$z_f-z_c\gtrsim r_{ns}\gg r_t$

$B_{dip}=7.1\cdot 10^{11}G$, $P=96ms$, $\tau=1.2\cdot 10^6$ years, $\chi=55°$

The polar cap luminosity for pulsar J2043+2740

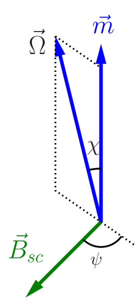

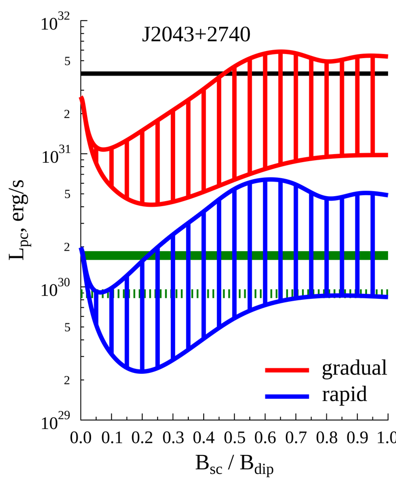

$$L_{pc}=\int e\Phi|_{z=z_c}\left.\frac{\Omega B}{2\pi ce}\right|_{z=0}\tilde\rho_+dS$$

$B_{dip}=7.1\cdot 10^{11}G$, $P=96ms$, $\tau=1.2\cdot 10^6$ years, $\chi=55°$

Upper limits of polar cap emission from [10] are shown by green lines, solid when we see one cap, dashed when we see both caps.

Emission of star surface taken from [11] is shown by black line.

The polar cap luminosity

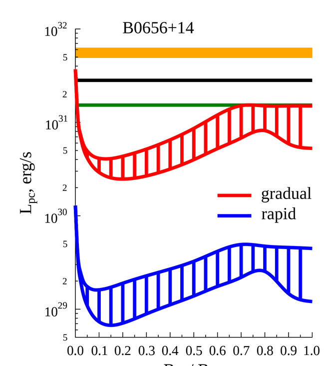

$B_{dip}=9.3\cdot 10^{12}G$, $P=0.385s$
$\tau=1.1\cdot 10^5$ years, $\chi=23°$
L_{pc} from [5] is shown by black line.
L_{pc} from [13] is shown by green line.
L_{pc} from [12] is shown by orange area

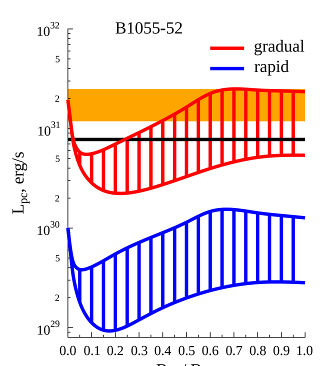

$B_{dip}=2.2\cdot 10^{12}G$, $P=0.197s$
$\tau=5.4\cdot 10^5$ years, $\chi=50°$
L_{pc} from [5] is shown by black line.
L_{pc} from [12] is shown by orange area

The polar cap luminosity

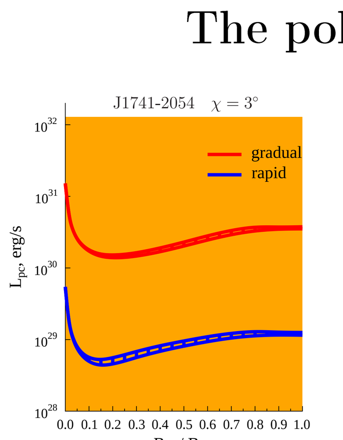

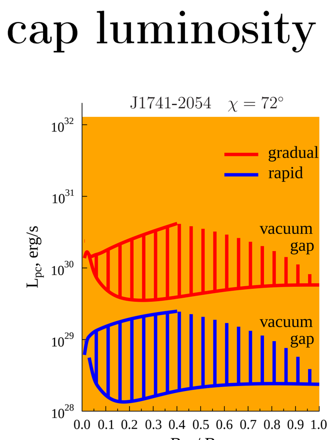

$B_{dip}=7.1\cdot 10^{11}G$, $P=96ms$, $\tau=1.2\cdot 10^6$ years
$\chi=3°$ (on left graph) and $\chi=72°$ (on right graph) [14]
Total surface luminosity L_{tot} from [15] is shown by orange area.

The polar cap luminosity

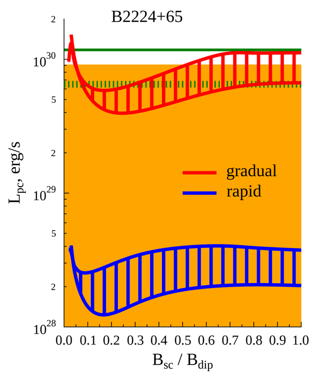

$B_{dip}=5.2\cdot 10^{12}G$, $P=0.68s$
$\tau=1.1\cdot 10^6$ years, $\chi=16°$
L_{pc} from [16] is shown by solid green line. Upper limit from [16] is shown by dashed green line, upper limit from [11] is shown by orange area.

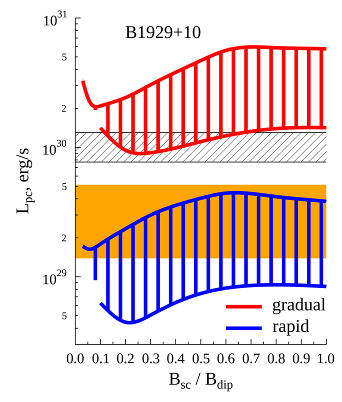

$B_{dip}=1.0\cdot 10^{12}G$, $P=0.23s$
$\tau=3\cdot 10^6$ years, $\chi=45°$
L_{pc} from [18] is shown by orange area. L_{pc} range from [12] is shown by black dashed area.

The polar cap luminosity

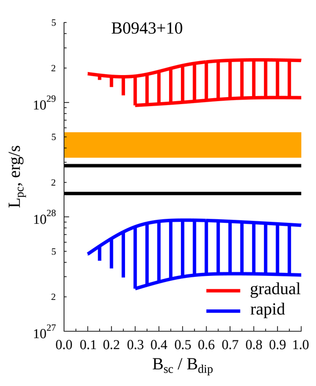

$B_{dip}=3.96\cdot 10^{12}G$, $P=1.097s$
$\tau=4.98\cdot 10^6$ years, $\chi=21°$
L_{pc} from [19] is shown by orange area.
$0.5L_{pc}$ range is shown by black lines.

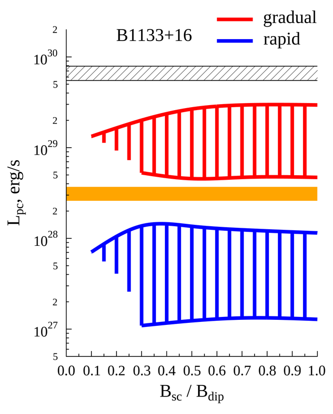

$B_{dip}=4.26\cdot 10^{12}G$, $P=1.19s$
$\tau=5.04\cdot 10^6$ years, $\chi=55°$
L_{pc} from [20] is shown by orange area.
L_{pc} range from [12] is shown by black dashed area.

The polar cap luminosity

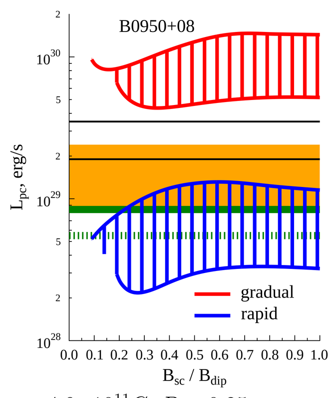

$B_{dip}=4.9\cdot 10^{11}G$, $P=0.25s$
$\tau=17.5\cdot 10^6$ years, $\chi=30°$
L_{pc} from [11] is shown by orange area and black lines. Upper limits from [10] are shown by green lines, solid when we see one cap, dashed when we see both caps.

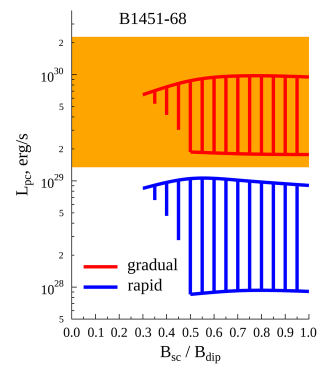

$B_{dip}=3.2\cdot 10^{11}G$, $P=0.26s$
$\tau=42.5\cdot 10^6$ years, $\chi=50°$
L_{pc} from [22] is shown by orange area

Conclusion

For some pulsars the gradual screening model predicts the polar cap heating which is larger than the observed polar cap luminosity.

Possible explanations:

1. Surface magnetic field $B_{surf}>10^{14}G$
   no free charge emission
   vacuum gaps, sparks [23]
2. Inner gaps occupy only small part of pulsar tube [24]
3. Large redshift $r_{ns}<2r_g$
4. Viscous forces at $z\sim r_t$ [25]
   Backflowing radiation [26, 27, 28]
   Radiation locked inside inner gaps [29, 30, 31]
   sound waves from neutron star interior [32]

We sincerely thank D.N. Sobyanin, I.F.Malov and V.A.Urpin for help, comments and usefull discussions, I.F. Malov, E.B.Nikitina for provided values of inclination angles, G.G.Pavlov for provided observational data, A.I. Chugunov, M.E.Gusakov, E.M.Kantor, Yu.A. Shibanov, D.A. Zyuzin, A.A. Danilenko, A.Yu.Kirichenko, M.A.Garasyov, V.M.Kontorovich, A.B.Flanchik, D.Mitra and D.M.Sedrakian for usefull discussions.
The work has been partly supported by the RFBR (project 13-02-00112) and by the State Program "Leading Scientific Schools of the Russian Federation" (grant NSh-294.2014.2).

References

[1] Arons J., Fawley W.M., Scharlemann E.T. // ApJ, V.**231** p.854 (1979)
[2] Harding A.K., Muslimov A.G. // ApJ, V.**556** p.987 (2001)
[3] Yu.E. Lyubarskii // A&A V.**261** p.544 (1992)
[4] J.A.Gil, G.I.Melikidze, D. Mitra // A&A, V. **388**, p. 235 (2002)
[5] A. Szary // arXiv:1304.4203
[6] R.N.Manchester et al // Astron. J., V. **129**, p. 1993 (2005) http://www.atnf.csiro.au/research/pulsar/psrcat
[7] I.F.Malov, E.B.Nikitina // Astronomy Reports, V. **55**, p.19 (2011)
[8] J.M. Rankin // ApJSS, V. **85**, p. 146 (1993)
[9] A.Noutsos et al // ApJ, V. **728**, p.77 (2011)
[10] W.Becker et al // ApJ, V. **615**, p.908 (2004)
[11] V.E. Zavlin, G.G. Pavlov // ApJ, V. **616**, p. 452 (2004)
[12] J.Gil et al. // ApJ, V. **686**, p. 497 (2008)
[13] G.Pavlov et al // *The Fast and the Furious: Energetic Phenomena in Isolated Neutron Stars, Pulsar Wind Nebulae and Supernova Remnants*, held 22-24 May, 2013 in Madrid, Spain. (2013)
[14] M. Pierbattista et al. // arXiv:1403.3849
[15] A.Karpova et al. // ApJ, V. **789**, id 97 (2014)
[16] C.Y.Hui, W.Becker // A & A, V. **467**, p.1209 (2007)
[17] C.Y.Hui et al // ApJ, V.**747**, p.74 (2012)
[18] Z.Misanovic et al // ApJ, V.**685**, p.1129 (2008)
[19] B. Zhang, D. Sanwal, G.G. Pavlov // ApJ, V. **624**, p. L109 (2005)
[20] O. Kargaltsev, G.G. Pavlov, G.P. Garmire // ApJ, V. **636**, p. 406 (2006)
[21] W.Becker et al. // ApJ, V.**615**, p.908 (2004)
[22] B.Posselt et al // ApJ, V.**749**, id 146 (2012)
[23] Gil J, Melikidze G I and Geppert U // A&A, V.**407**, p.315 (2003)
[24] S. Shibata // ApJ, V.**378**, p.239. (1991)
[25] S.Shibata et al // MNRAS, V.**295**, L53 (1998)
[26] G.Melikidze, J.Gil // Chin. J. Astron. Astrophys., V.**6**, Suppl. 2, p.81 (2006)
[27] J.Dyks et al // Chin. J. Astron. Astrophys., V.**6**, Suppl. 2, p.85 (2006)
[28] D.Lomiashvili et al // arXiv:0709.2019 (2007)
[29] V.M.Kontorovich, A.B.Flanchik // JETP Letters, V.**85**, p. 267 (2007)
[30] V.M.Kontorovich, A.B.Flanchik // JETP, V. **106**, p.869 (2008)
[31] V.M.Kontorovich, A.B.Flanchik // Astrophysics and Space Science, V. **345**, p. 169 (2013)
[32] D.M.Sedrakyan // "The Modern Physics of Neutron Stars and Relativistic Gravity" Yerevan, Armenia, September 18-21, 2013